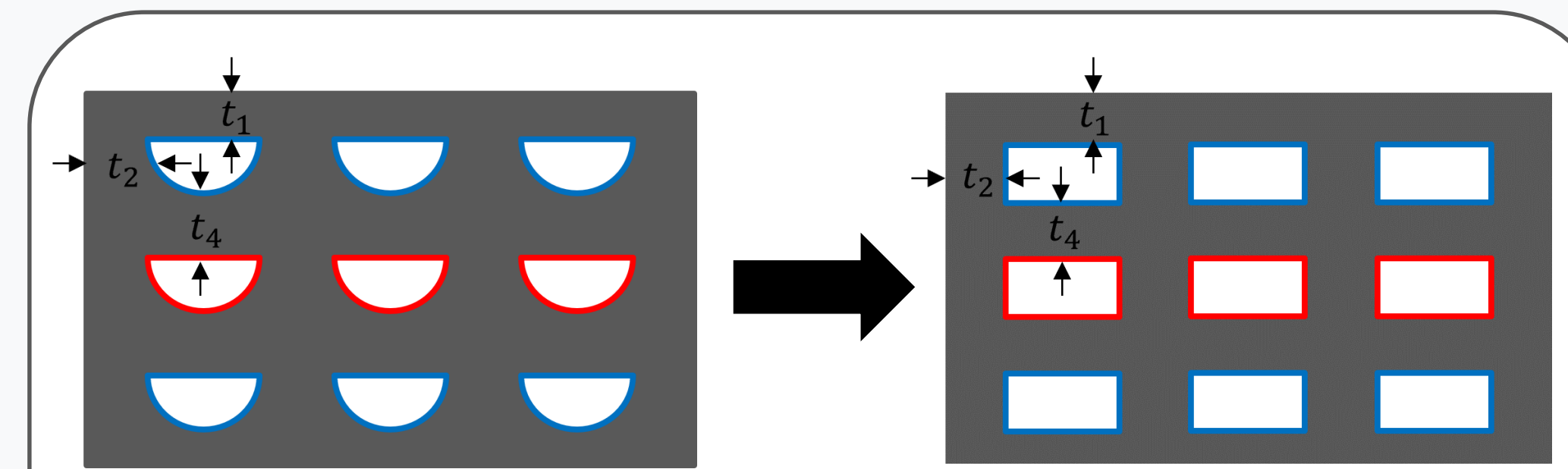
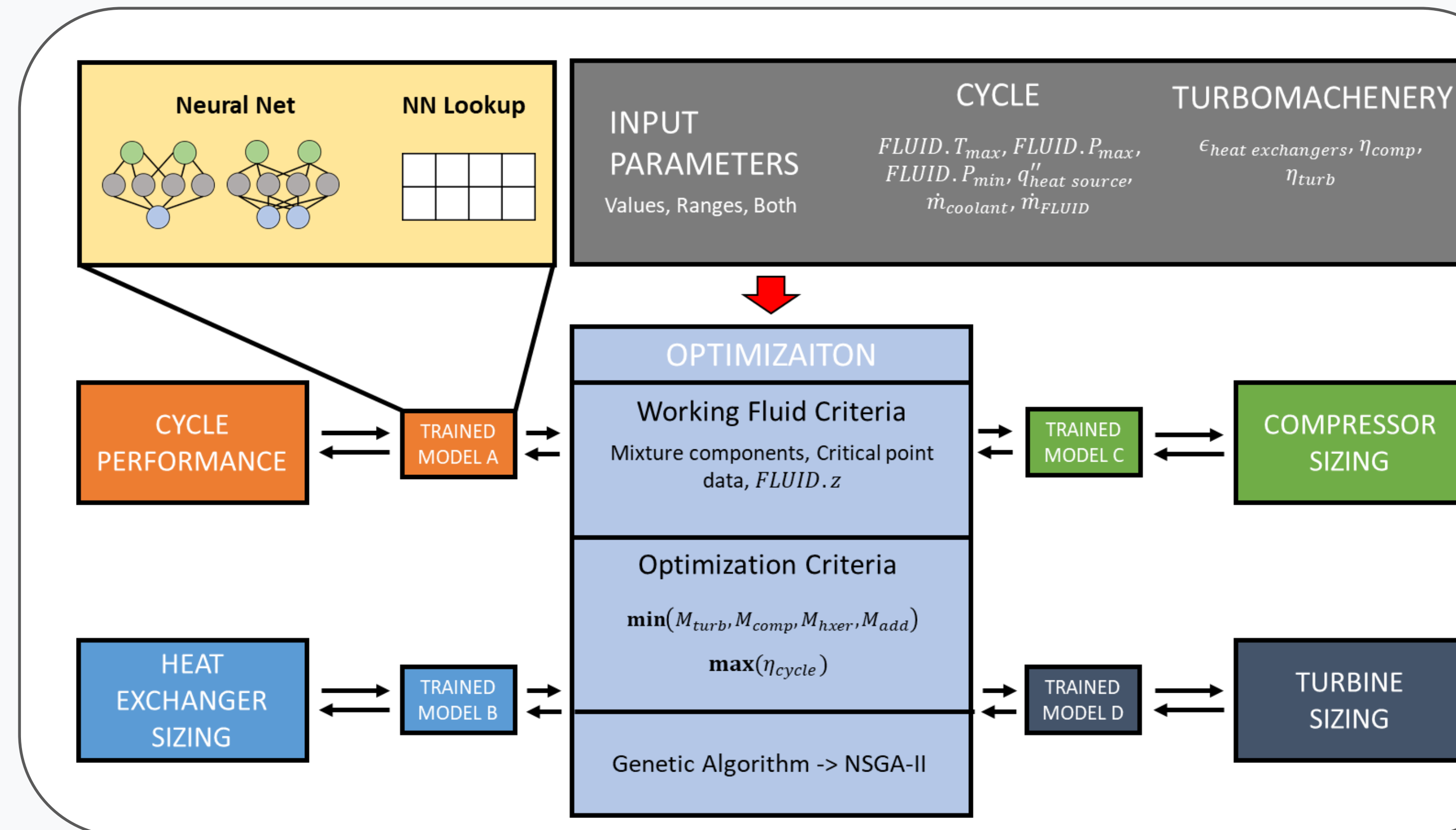


Thermomechanical analysis of printed circuit heat exchangers for optimization of supercritical CO₂ based power cycles in concentrated solar power

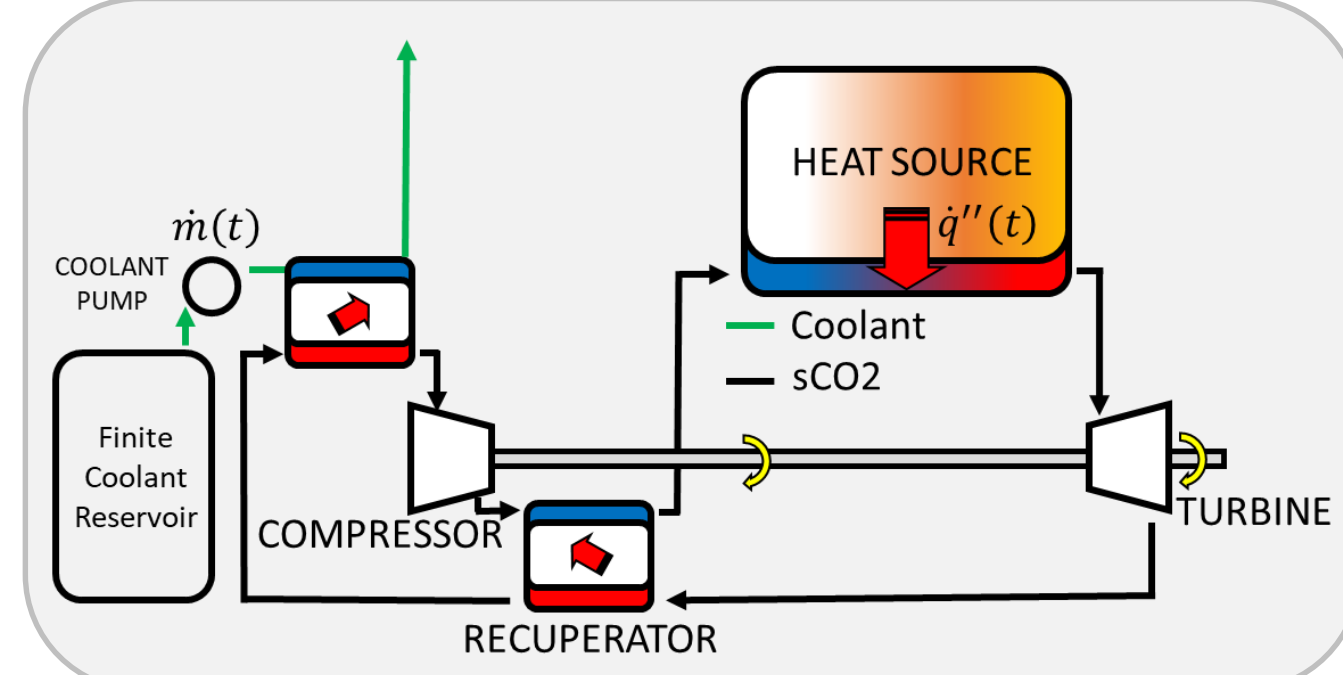
Christopher J. Hyland¹, Joshua M. Petry¹, Robert Lowe¹, Justin DeMar², Andrew J. Schrader^{1*} (University of Dayton¹, Wright Patterson Air Force Base²)

This study explores the development of cost functions for supercritical carbon dioxide (sCO₂) power cycles, specifically designed for thermal-reservoir limited applications such as concentrated solar power facilities. Utilizing a multi-objective evolutionary algorithm, a systems-level thermodynamic analysis was conducted, focusing on various cycle and turbomachinery parameters. The analysis integrated cycle thermodynamics with turbomachine and heat exchanger sizing algorithms, leading to predictions of required component sizing for optimal system performance. Additionally, the study assessed the implications of thermal reservoir constraints on cycle efficiency, considering environmental factors like high heat coolant inlet temperatures. The research also evaluated printed circuit heat exchangers, considering variables such as channel number (Nc), number of plates (Np), channel length (Lc), hydraulic diameter (Dh), and channel path, alongside variation in material choices and design considerations impacting component lifetime, particularly focusing on creep-rupture phenomena.



The Heat Exchanger can be simplified to a rectangular model from a semi-circular one. Simplified stress equations are essential for developing and validating models in the thermal design of Printed Circuit Heat Exchangers. They facilitate the identification of key geometrical parameters and enable a more feasible approach to evaluate the mechanical strength and stresses in these structures.

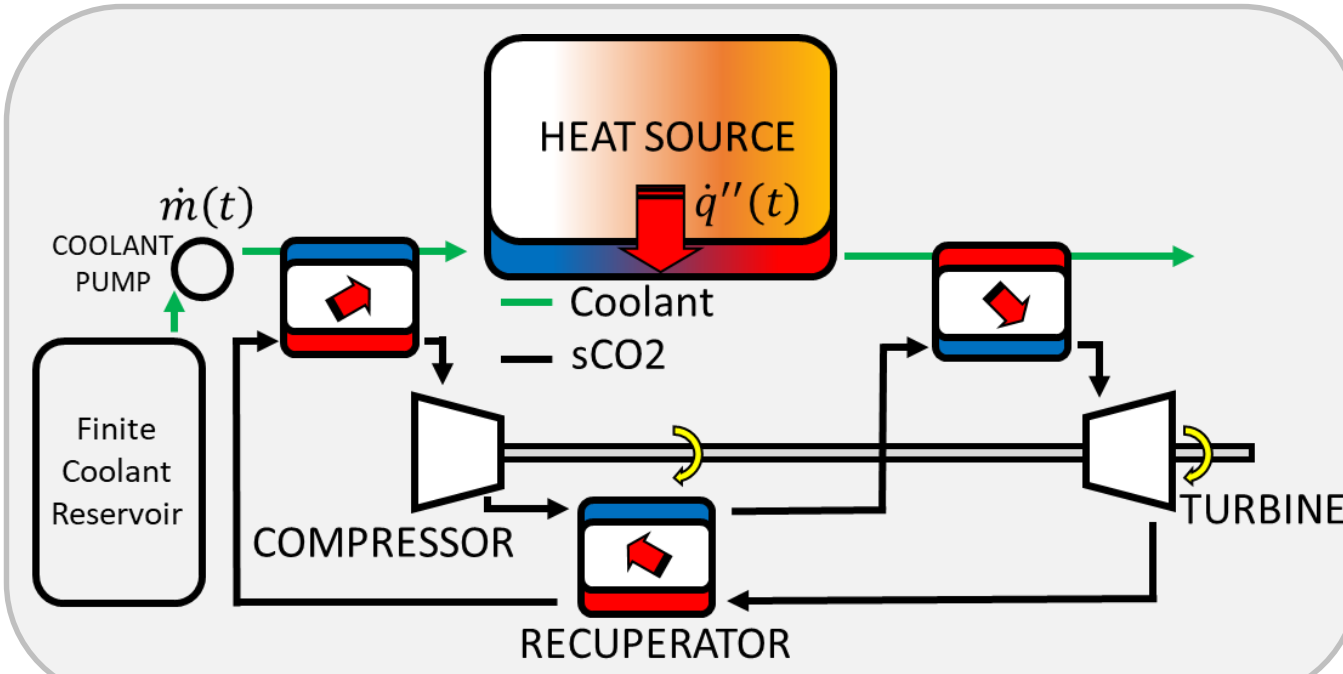
Direct Heating Recuperation Cycle



Cycle Max Temp:
[600,900] K
Coolant Inlet Temp:
[275,315] K
Compressor eff.:
[0.7,0.9]
Turbine eff.:
[0.7,0.9]
Heat exchanger ε:
[0.4,0.9]
Fluid mass flow rate:
[2,18] kg/s
Coolant mass flow rate:
[3,10] kg/s

Direct Heating Non-Recuperated Cycle: non-recuperated direct heating cycle variation

Indirect Heating Recuperation Cycle



Q.Source
DH-RC: [0.27,7.6] MW
DH-NRC: [0.35,12.5] MW
IH-RC: [2.0,15.8] MW
IH-NRC: [1.3,14.8] MW

Indirect Heating Non-Recuperated Cycle: non-recuperated indirect heating cycle variation

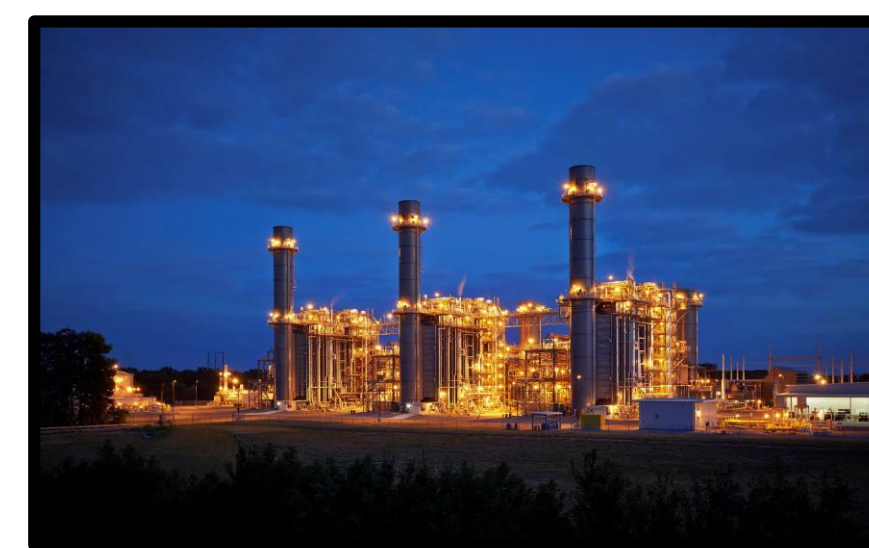
The proposed simulation and optimization framework is designed to encompass a comprehensive set of closed-loop Brayton cycle architectures, illustrated initially by four generic cycle variations. This framework aims to facilitate faster and more efficient optimization of Brayton cycles tailored to specific application requirements. By incorporating a broad spectrum of cycle architectures, the framework ensures scalability and adaptability, significantly enhancing the optimization process for most applications

Distribution Statement A. Approved for public release: distribution is unlimited.

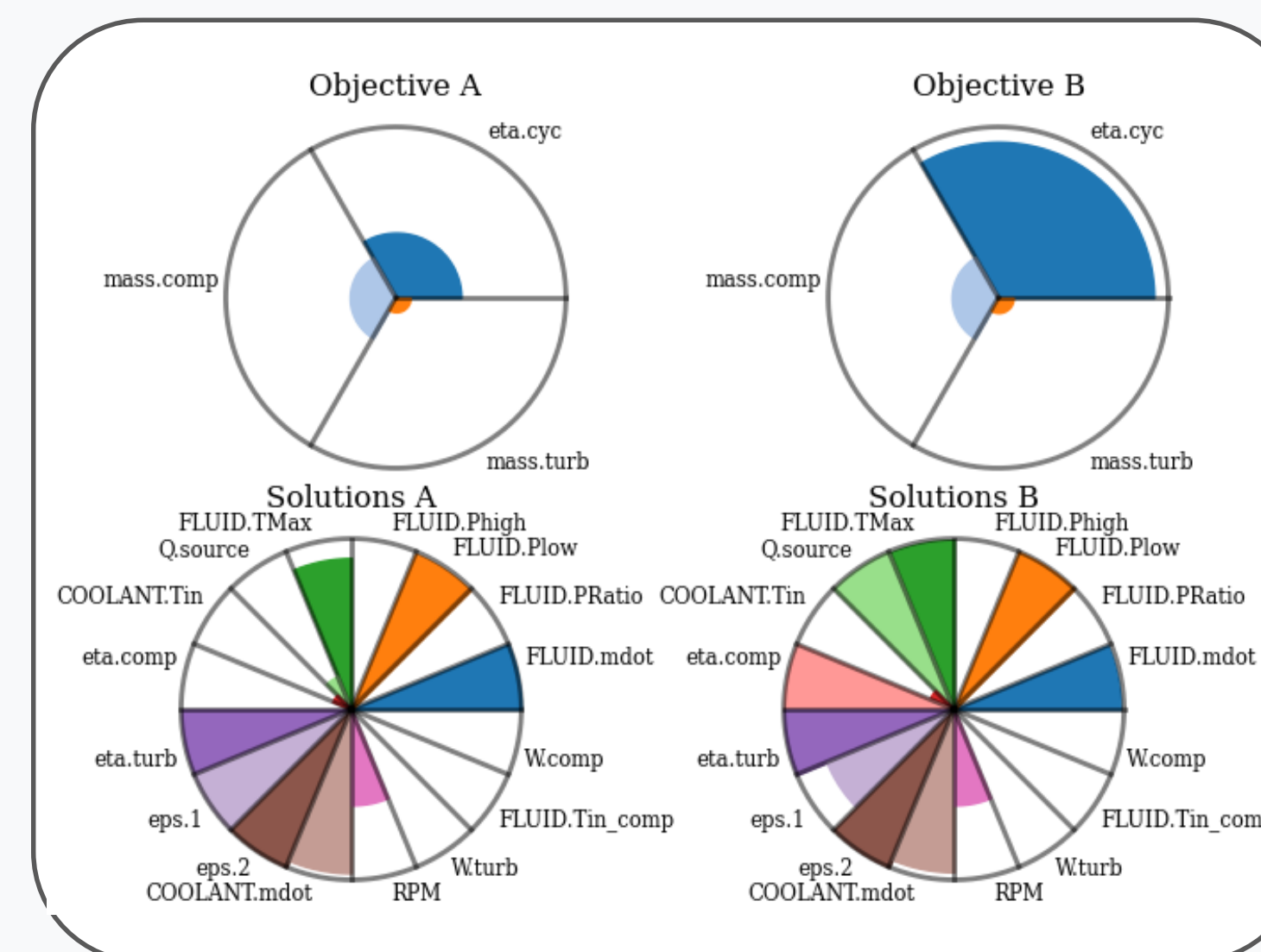
Concentrated Solar Power



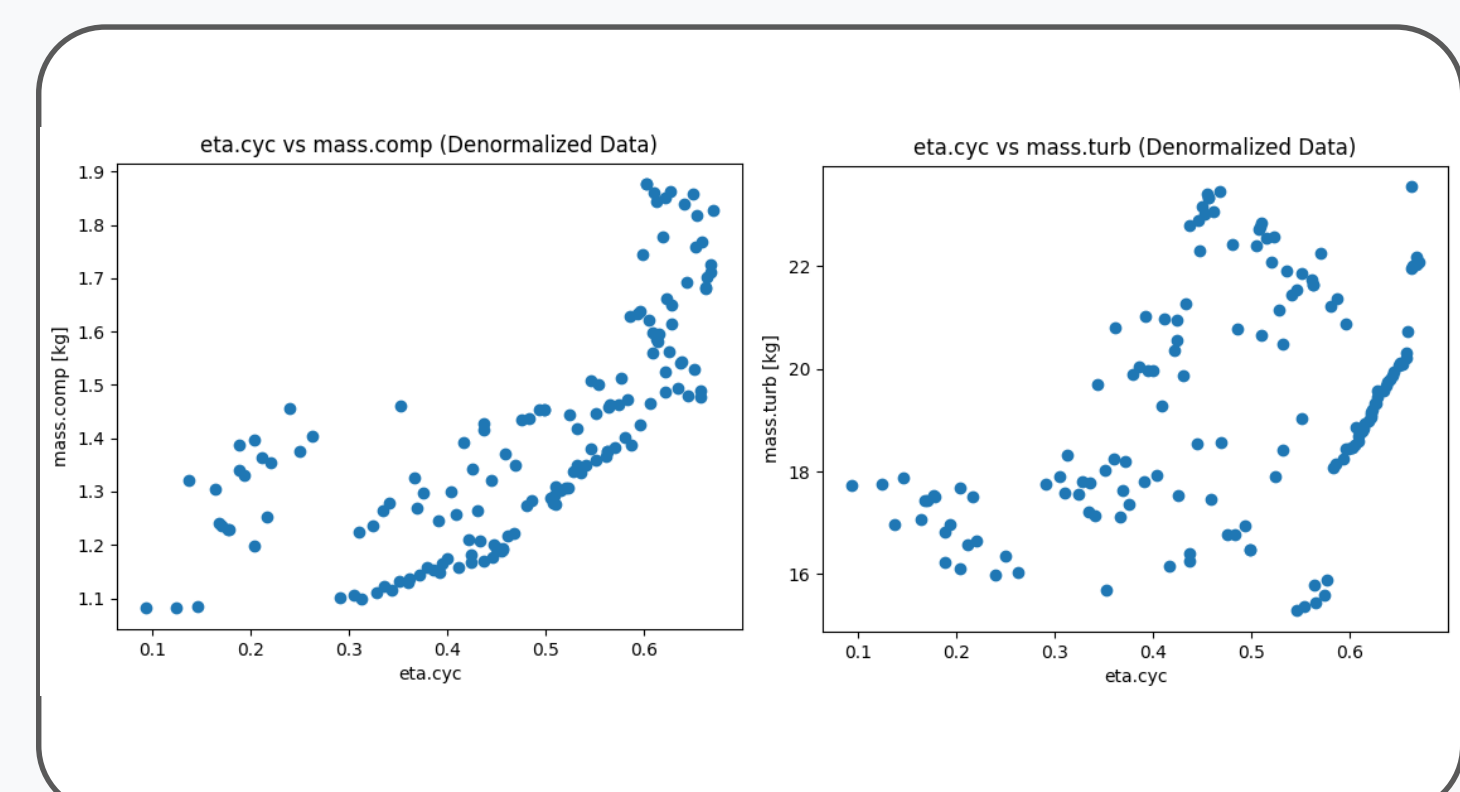
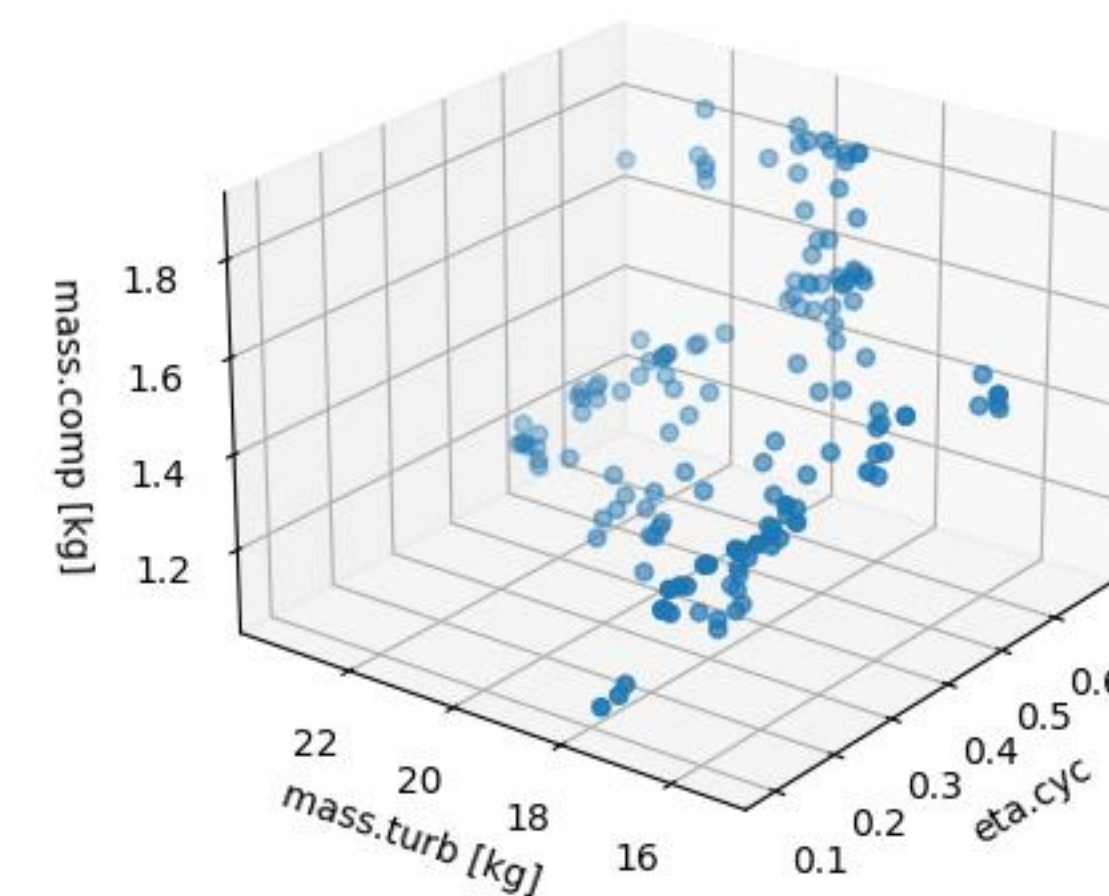
Non-renewable energy sources



Onboard power systems

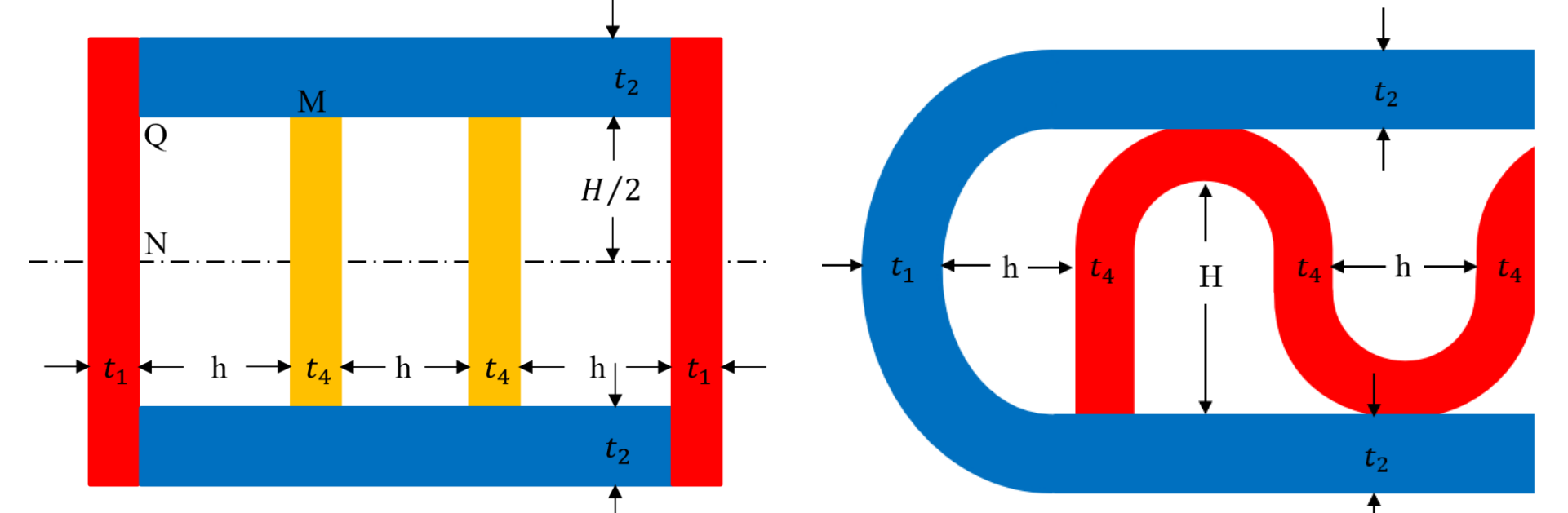


3D Scatter Plot of Objectives (Denormalized Data)



Optimization studies have been performed for the Recuperated Direct-Heating Brayton Cycle with optimization criteria of minimizing component masses and maximizing cycle efficiency. Two-dimensional and three-dimensional pareto plots are provided to demonstrate the wide variety of potentially optimized cycles. Petal plots of normalized solution objectives were initially developed for two representative 'optimal' solutions to further evaluate the solution variation. While a number of candidate optimal solutions exist, further tuning of the optimization criteria and application-specific restrictions are required and currently being investigated.

Boiler Code Stress Analysis



Short Side Equations

$$(S_T)_N = \frac{Ph}{2t_1} \left\{ 3 - \left[\frac{6 + K(11 - \alpha^2)}{3 + 5K} \right] \right\} + \frac{Pc}{24I_1} \left[-3H^2 + 2h^2 \left(\frac{3 + 5\alpha^2 K}{3 + 5K} \right) \right]$$

$$(S_T)_Q = \frac{Ph}{2t_1} \left\{ 3 - \left[\frac{6 + K(11 - \alpha^2)}{3 + 5K} \right] \right\} + \frac{Ph^2 c}{12I_1} \left(\frac{3 + 5\alpha^2 K}{3 + 5K} \right)$$

Long Side

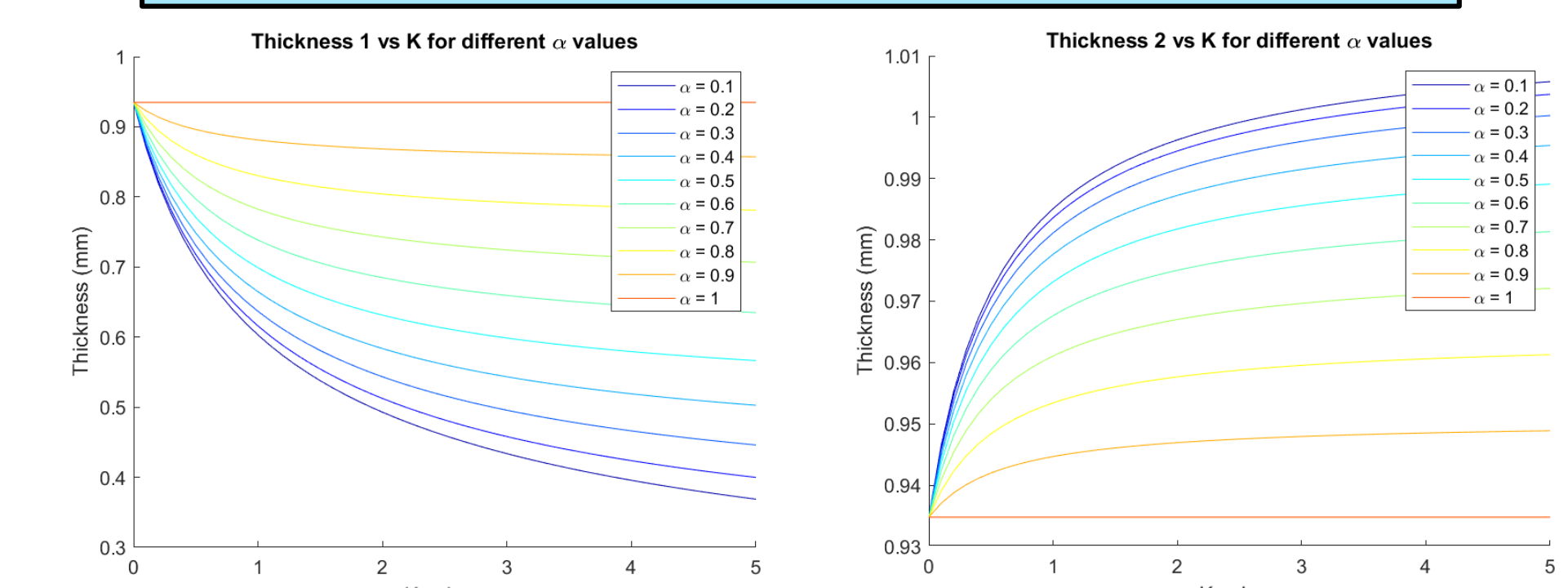
$$(S_T)_M = \frac{PH}{2t_2} + \frac{Ph^2 c}{12I_2} \left(\frac{3 + K(6 - \alpha^2)}{3 + 5K} \right)$$

$$(S_T)_Q = \frac{PH}{2t_2} + \frac{Ph^2 c}{12I_2} \left(\frac{3 + 5\alpha^2 K}{3 + 5K} \right)$$

Stay Plate

$$S_T = \frac{Ph}{2t_4} \left[\frac{6 + K(11 - \alpha^2)}{3 + 5K} \right]$$

Sizing Code Equation Comparison



Thickness 1, designated as T1, exhibits a decreasing trend as K increases for a given alpha smaller than 1. The opposite can be said for T2. T2 also exhibits a smaller rate of change because of the K(6-α²) term.